UC Davis
UC Davis Previously Published Works

Title

Nitrate pollution source apportionment, uncertainty and sensitivity analysis across a rural-urban river network based on δ 15N/δ 18O-NO3 − isotopes and SIAR modeling

Permalink

https://escholarship.org/uc/item/7kc6w82n

Authors

Ji, Xiaoliang
Shu, Lielin
Chen, Wenli
et al.

Publication Date

2022-09-01

DOI

10.1016/j.jhazmat.2022.129480

Peer reviewed

Nitrate pollution source apportionment, uncertainty and sensitivity analysis across a rural-urban river network based on $\delta^{15}N/\delta^{18}O\text{-}NO_3^-$ isotopes and SIAR modeling

Xiaoliang Ji [a,c], Lielin Shu [a], Wenli Chen [a], Zheng Chen [a,c], Xu Shang [a,c], Yue Yang [b,*], Randy A. Dahlgren [a,d], Minghua Zhang [a,c,d,**]

[a] *Key Laboratory of Watershed Science and Health of Zhejiang Province, School of Public Health and Management, Wenzhou Medical University, Wenzhou 325035, China*
[b] *Zhejiang Provincial Key Laboratory for Water Environment and Marine Biological Resources Protection, College of Life and Environmental Science, Wenzhou University, Wenzhou 325035, China*
[c] *Southern Zhejiang Water Research Institute, Wenzhou 325035, China*
[d] *Department of Land, Air and Water Resources, University of California, Davis, CA 95616, USA*

HIGHLIGHTS

- Sensitivity analysis was performed firstly for SIAR modeling.
- $\delta^{15}N/\delta^{18}O\text{-}NO_3^-$ and SIAR identified MS as the possible major nitrate source.
- Uncertainties of source contributions decreased in the order: NF > SN > MS > > AD.
- Model results are most sensitive to isotopic composition of major nitrate source.

GRAPHICAL ABSTRACT
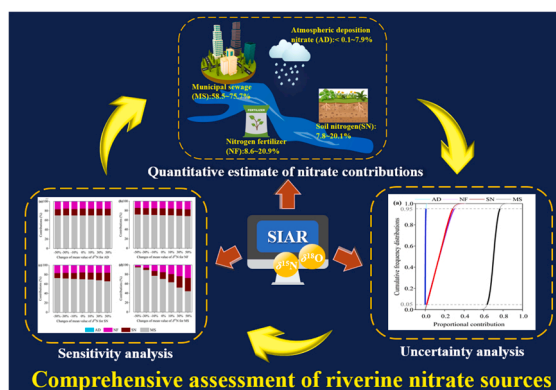
ARTICLE INFO

Editor: Dr. B. Lee

ABSTRACT

Nitrate pollution is of considerable global concern as a threat to human health and aquatic ecosystems. Nowadays, $\delta^{15}N/\delta^{18}O\text{-}NO_3^-$ combined with a Bayesian-based SIAR model are widely used to identify riverine nitrate sources. However, little is known regarding the effect of variations in pollution source isotopic composition on nitrate source contributions. Herein, we used $\delta^{15}N/\delta^{18}O\text{-}NO_3^-$, SIAR modeling, probability statistical analysis and a perturbing method to quantify the contributions and uncertainties of riverine nitrate sources in the Wen-Rui Tang River of China and to further investigate the model sensitivity of each nitrate source. The SIAR model

Uncertainty analysis
Sensitivity analysis

confirmed municipal sewage (MS) as the major nitrate source (58.5–75.7%). Nitrogen fertilizer (NF, 8.6–20.9%) and soil nitrogen (SN, 7.8–20.1%) were also identified as secondary nitrate sources, while atmospheric deposition (AD, $<$0.1–7.9%) was a minor source. Uncertainties associated with NF ($UI_{90} = 0.32$) and SN ($UI_{90} = 0.30$) were high, whereas those associated with MS ($UI_{90} = 0.14$) were moderate and AD low ($UI_{90} = 0.0087$). A sensitivity analysis was performed for the SIAR modeling and indicated that the isotopic composition of the predominant source (i.e., MS in this study) had the strongest effect on the overall riverine nitrate source apportionment results.

1. Introduction

Increasing nitrate (NO_3^-) concentration in river systems is a global environmental and human health concern resulting from anthropogenic perturbations to the global nitrogen (N) cycle. Nitrate is a key factor attributing to human health risks, such as "blue baby" syndrome, miscarriages, esophagus/stomach cancer and eutrophication/hypoxia in aquatic ecosystems (Burow et al., 2010; Carey et al., 2011; Hord, 2011; Nestler et al., 2011; World Health Organization, 2011). Riverine NO_3^- concentrations are attributed to several potential pollution sources, such as atmospheric deposition nitrate (AD), nitrogen fertilizer (NF), soil nitrogen (SN), municipal sewage (MS) and industrial wastewater, as well as multiple transformations occurring within the nitrogen cycle (e. g., nitrification and denitrification) (Kendall et al., 2007; Lu et al., 2015; Jin et al., 2018). To effectively control and remediate riverine NO_3^- pollution, it is of fundamental importance to quantitatively evaluate sources and identify key transformation processes affecting variations in nitrate concentrations at the watershed scale.

In the past few decades, several nutrient source apportionment models have been developed for application in a variety of aquatic systems. These models, range from simple export coefficient models or their modified formats (Johnes, 1996; Wang et al., 2020a), to statistical regression models (e.g., SPARROW model; Smith et al., 1997), to complex geographic information system (GIS)-based models (see Supplementary materials for detailed information regarding source apportionment approaches/models and their perceived advantages). Common GIS-based models include the Storm Water Management Model (Rossman, 2015), Hydrological Simulation Program-Fortran (Donigian et al., 1984), and the most widely used Soil and Water Assessment Tool (Arnold and Fohrer, 2005).

Despite the abundance of modeling tools, riverine nutrient source apportionment remains a challenge, especially due to insufficient data for parameterization and calibration/verification. For example, GIS-based models typically require large and complex parameterization datasets to mathematically simulate hydrological and coupled nutrient transformation/transport processes in terrestrial-riverine systems, which makes their application difficult. Conversely, export coefficient models and statistical regression models generally provide a simplified approach to assess nutrient source inputs from the watershed to rivers. However, they also require information about watershed and river attributes (e.g., land-use type, quantity of livestock and poultry, and river flow), as well as nutrient discharge from industries and sewage treatment facilities. In addition, the failure of effective hydrological simulation models for plain river networks render them often unsuitable for plain river systems. Moreover, the parameters inherent in export coefficient models are often obtained from the literature or estimated by empirical methods, and thus contain large uncertainties, especially when applied to different watershed/river systems. The statistical regression SPARROW model is based on spatial statistics while lacking an explicit description of pollution source dynamics. Finally, GIS-based models have a difficult learning-curve and require considerable expertise for effective deployment.

Analysis and interpretation of stable nitrate isotopes (^{15}N and ^{18}O) provide a promising approach for assessing the sources and fate (i.e., transformations/transport) of riverine NO_3^- based on different nitrate pollution sources with unique stable isotopic characteristics and nitrogen cycling processes with specific isotopic fractionation signatures (Biddau et al., 2019; Hu et al., 2019; Torres-Martínez et al., 2021a). Advantages of this approach include less ancillary information requirements, easy operation, high precision and direct identification of pollution sources. Commonly, the stable nitrogen isotope of nitrate ($\delta^{15}N\text{-}NO_3^-$) is more appropriate for identifying NO_3^- derived from soil nitrogen, manure/sewage and nitrogen fertilizer (Kendall and McDonnell, 1998). In contrast, the stable oxygen isotope of nitrate ($\delta^{18}O\text{-}NO_3^-$) is effective in differentiating NO_3^- originating from microbial nitrification of reduced nitrogen forms, nitrate-bearing fertilizer and atmospheric deposition (Kendall and McDonnell, 1998; Mayer et al., 2001). An integration of $\delta^{15}N/\delta^{18}O\text{-}NO_3^-$ with model analyses or simulation has been successfully applied in many scenarios, such as rivers, reservoirs, lakes, estuaries, and groundwater, to trace nitrate sources and transformations (Ji et al., 2017; Soto et al., 2019; Jin et al., 2020; Shang et al., 2020; Wang et al., 2020b).

Recently, a Bayesian-based mixing model known as the Stable Isotope Analysis in R (SIAR) model has attracted a great deal of interest since it provides quantitative information regarding NO_3^- source apportionment (Parnell et al., 2010; Yang et al., 2013; Shang et al., 2020). For example, Xue et al. (2012) utilized the SIAR model to assess the proportional contributions of five potential nitrate sources in surface waters in Flanders (Belgium), with the results identifying manure and sewage as the largest NO_3^- contributors. Similarly, Divers et al. (2014) employed the SIAR model to quantify the proportional contributions of nitrate sources in an urban stream in Pittsburgh (USA), finding that up to 94% of stream water nitrate originated from sewage sources during baseflow periods and an average of 67% during stormflow. Likewise, Soto et al. (2019) used nitrate isotopes and the SIAR model to identify nitrate sources in the Assiniboine and Red rivers (Canada). Their results showed that manure and/or wastewater discharge contributed 62% of the nitrate in the Assiniboine River, whereas inorganic agricultural fertilizers contributed 40% of nitrate in the Red River.

Although the SIAR model offers a number of merits and has been successfully deployed, uncertainties in nitrate source apportionment are inevitable due to the relatively wide isotopic ranges of some nitrate sources and isotopic fractionations occurring during nitrogen transformation processes (e.g., nitrification and denitrification) (Liu et al., 2013; Zhang et al., 2018). Fortunately, the SIAR model allows quantification of the model uncertainty associated with the uncertainty of input data (Divers et al., 2014; Ji et al., 2017; Ju et al., 2022). The SIAR model adopts a Monte Carlo sampling approach for each end-member (i. e., pollution source), allowing non-Gaussian and/or observed distributions. Each sample is then applied to estimate fractions (proportional contributions) of end-members and the sampling is repeated, generating a probability distribution of proportional contributions (Yang et al., 2013). One important component of nitrate pollution source apportionment using the SIAR model is to determine the uncertainty of model results and the effect of input data uncertainty on the model results. However, the effect of variations in pollution source isotopic composition on nitrate source contributions when using nitrate isotopes and the SIAR model has not been thoroughly investigated.

Given the above considerations, this study systematically collected water samples from a typical rural-urban river network known as the Wen-Rui Tang River (China) in four seasons (April, June, September and January 2019–2020). Hydrochemistry and dual nitrate isotopes ($\delta^{15}N/$

δ^{18}O-NO$_3^-$) of quarterly sampled river water were analyzed to: (1) trace the sources and transformations of riverine nitrate in a typical coastal plain river network using δ^{15}N/δ^{18}O-NO$_3^-$ isotope analysis and subsequent SIAR modeling; (2) identify the inherent uncertainty of nitrate pollution source apportionment through probability statistical analysis; and (3) investigate the relative change in nitrate source contributions resulting from different nitrate source isotopic composition (i.e., the impact of input data uncertainty on the SIAR model output) via a perturbing method. Results of this study will inform local environmental and water resource agencies with quantitative information on nitrate source apportionment that will provide a better scientific basis for developing nitrogen pollution control and remediation strategies for maintaining healthy river systems.

2. Materials and methods

2.1. Study area

The Wen-Rui Tang (WRT) River watershed (27°51´–28°02´N, 120°28´–120°46´E) in eastern China was selected as the study site due to its eutrophic condition and its need for nutrient remediation actions (Fig. 1). The WRT River is a typical coastal plain river network spanning the rural-urban interface in the densely populated Wenzhou city (~9 million population), Zhejiang province (China), with an area of 740 km^2. The river originates from the Lishui Mountains, and meanders through rural zones with agricultural lands, and a densely populated urban area before discharging into the East China Sea. Its mainstream is ~34 km long and associated tributaries/canals are ~1200 km long with many hardened waterways. The WRT River watershed has a subtropical oceanic climate with annual rainfall levels of 1500–1900 mm and ~70% of precipitation falling between April and September. Natural vegetation, built land (including residential and industrial area) and agriculture are the dominant land-use categories, accounting for ~40%, ~38%, and ~18% of the entire watershed. Due to the seasonal precipitation pattern and plain topography (i.e., low river gradient), the WRT River

has stagnant to low flows (<0.05 m/s) for much of the year, except when the flood gates to the Ou River are open during high flow events (>2 m/s; typhoons) and the river flows directly into the Ou River (Wang et al., 2018).

2.2. Sampling and analytical methods

In this study, 24 sampling sites were selected across the WRT River watershed (Fig. 1). To study seasonal variability in hydrochemical and isotopic parameters, four sampling events were carried out on a quarterly basis. River water samples were collected in April (spring − moderate flow), June (summer − high flow), September (autumn − moderate flow) 2019 and January (winter − low flow) 2020. For each sampling event, 24 river water samples were collected between 9:00 a.m. and 16:00 p.m. in one day. Dissolved oxygen (DO) was recorded in situ at each sampling site using a multi-parameter water-quality sonde (YSI-EXO2, Xylem, USA). Water samples were collected from 30-cm below the water surface in the center of a well-mixed channel segment using a hydrophore sampler. Water samples were immediately placed in pre-washed 500 mL polyethylene bottles and subsequently transported with ice packs in a foam box to our lab at the university. To obtain the site-specific isotopic compositions of potential N pollution sources, daily-based precipitation ($n = 15$), top soil (1–10 cm depth, $n = 32$) and chemical fertilizer (i.e., ammonium and urea, $n = 10$) samples were collected within the WRT watershed.

In the laboratory, water sample was filtered through 0.45 μm mixed cellulose ester membrane filter (Tengjin, Tianjin, China) for determination of dissolved inorganic nitrogen concentrations within 12 h of sampling. Three nitrogen parameters, namely, ammonia-nitrogen (NH$_4^+$), nitrite-nitrogen (NO$_2^-$), and nitrate-nitrogen (NO$_3^-$) were analyzed within a week of sample collection. Specifically, NO$_3^-$, NH$_4^+$, and NO$_2^-$ were analyzed using a continuous-flow analyzer (Auto-analyser-3, Seal, German) with limit of detection (LOD) of ~0.003 mg/L for dissolved inorganic nitrogen (NO$_3^-$, NH$_4^+$, NO$_2^-$). Chemical fertilizer and soil samples were air-dried, homogenized and passed through a 149-
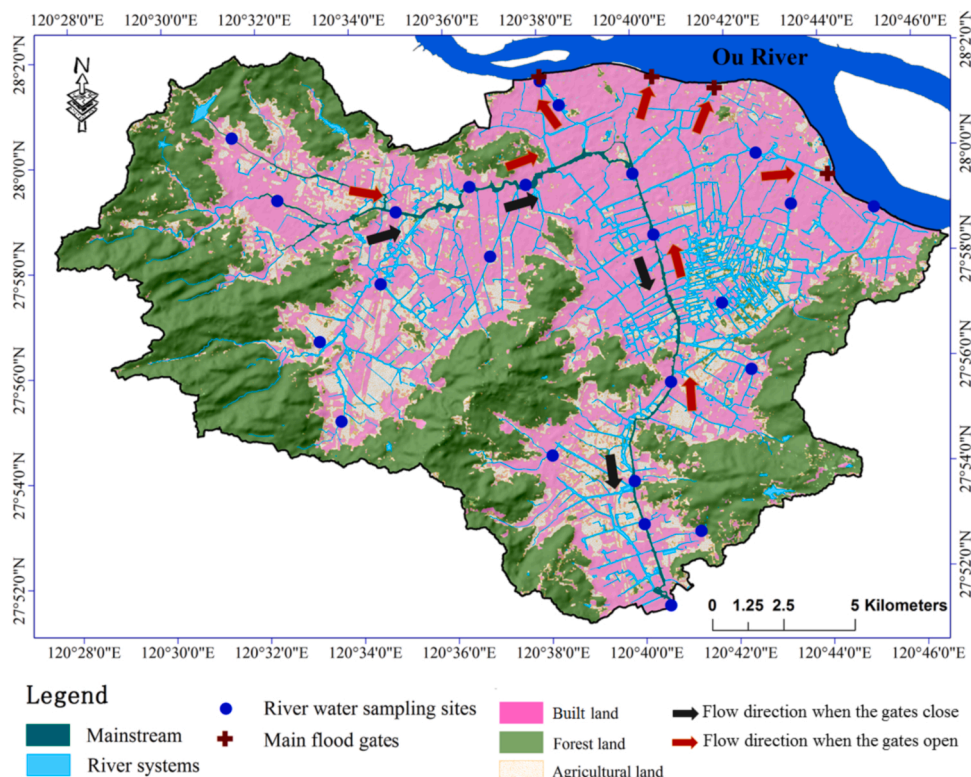

Fig. 1. Sampling sites of the Wen-Rui Tang River watershed.

µm screen. Powdered samples were stored in HDPE bags. All samples for stable isotope analysis were transported with ice packs in the foam box to the Chinese Academy of Agricultural Sciences (China). δ^{15}N/δ^{18}O-NO$_3^-$ analysis followed the bacteria denitrifier method presented by Sigman et al. (2001) and Casciotti et al. (2002). This method uses the denitrifying bacteria known as *Pseudomonas aureofaciens*, which naturally lack the gaseous nitrous oxide (N$_2$O) reductive activity, to convert NO$_3^-$ to N$_2$O. The N$_2$O was purified through a Thermo pre-concentrator system and then analyzed for δ^{15}N/δ^{18}O-N$_2$O using a Thermo Delta V isotope ratio mass spectrometer. Powdered samples were placed in tin cups and delivered to a Elementar elemental analyzer coupled to a IsoPrime isotope ratio mass spectrometer for nitrogen isotope analysis. Three international nitrate standards (USGS-32, USGS-34 and USGS-35) were employed to calibrate the measured δ^{15}N/δ^{18}O values. The δ^{15}N value is expressed in parts per thousand (‰) relative to atmospheric N$_2$ and the analysis precision is $\pm$ 0.2‰; the δ^{18}O value is expressed in ‰ relative to Vienna Standard Mean Ocean Water and the analysis precision is $\pm$ 0.5‰ (Kendall et al., 2007).

2.3. Stable Isotope Analysis in R (SIAR) model

To calculate NO$_3^-$ source contributions in the WRT River watershed, a Bayesian-based SIAR model was implemented. The equations of the system model can be expressed as follows (Parnell et al., 2010):

$$\left.\begin{array}{l} X_{ij} = \sum_{k=1}^{k} P_k \left(S_{jk} + C_{jk}\right) + \varepsilon_{ij} \\[2mm] S_{jk} \sim N\left(\mu_{jk}, \omega_{jk}^2\right) \\[2mm] C_{jk} \sim N\left(\lambda_{jk}, \tau_{jk}^2\right) \\[2mm] \varepsilon_{ij} \sim N\left(0, \sigma_j^2\right) \end{array}\right\} \quad (1)$$

where X_{ij} represents isotopic signature j (δ^{15}N/δ^{18}O-NO$_3^-$ in this study) of the mixture i (river water samples in this study; $i = 1, 2, 3...N$); P_k denotes the estimated proportional contribution of source k (i.e., AD, NF, SN, and MS), which obeys a Dirichlet distribution; S_{jk} refers to the isotope j of source k; C_{jk} is the isotopic fractionation caused by nitrogen transformations for isotope j of source k; and ε_{ij} represents the residual error, which refers to the unquantified variation among individual mixtures. Herein, the SIAR model was implemented by the Stable Isotope Analysis in R software package (SIAR V4) running on the R platform (version 3.1.2, R Core Team, 2019). Operational parameters regarding SIAR modeling i.e., iteration maintainer, sample interval, burn-in and run iterations were set as 30,000, 15, 50,000, and 500,000, respectively.

2.4. Uncertainty analysis

A large number of uncertainties exist in nitrate source apportionment arising mainly from spatio-temporal variations in the isotopic fingerprint of the pollution sources and isotopic fractionation during biochemical nitrogen cycling processes. Herein, we used a probability statistical method to assess the uncertainties associated with the simulation results of the SIAR model, as follows: (1) sorting of the 30,000 (iteration maintainer) groups of each kind of pollution contribution value in order; (2) assigning a frequency to each pollution contribution value as 1/30,000, and summing the frequency of each source to equal 1; (3) determining the cumulative probability distributions of the proportional contributions from different potential nitrate sources using the proportional contribution as the *x*-axis and cumulative frequency as the *y*-axis. The cumulative frequency profile is capable of providing the quantile value of the simulated value, i.e. $p \times 100/30,000\%$ is the quantile point of the pth simulated value; and (4) calculating an uncertainty index (UI_{90}) to characterize the uncertainty strength. The UI_{90} is

defined as the proportional contribution of the 0.95 cumulative frequency distribution minus that at the 0.05 cumulative frequency distribution, and then divided by 0.9. Additional details regarding the UI_{90} calculation are documented in Ji et al. (2017) and Torres-Martínez et al. (2021a), (2021b).

2.5. Sensitivity analysis

The SIAR model uses the mean and standard deviation of δ^{15}N and δ^{18}O for each pollution source as the calculated end-members. In this study, a perturbing method was employed to evaluate the sensitivity (the effect extent of different changes in input variables on the SIAR outputs) of isotopic signatures for different pollution sources. This algorithm changes the value of one input while keeping the others intact. The variabilities of the model output against that of the input variables are recorded. The most important (i.e., most sensitive) input variable is the variable that creates the largest change in the results. With the aim of quantifying the sensitivity of each input end-member, we established different simulation scenarios via changing mean values of δ^{15}N for different sources by $\pm$ 50%, $\pm$ 30%, $\pm$ 10% and 0%. In this study, the sensitivity of δ^{18}O was not investigated since the δ^{18}O values for several pollution sources were obtained from established nitrification theory rather than actual measurements.

3. Results and discussion

3.1. Overview of water quality

Overall water quality impairment was closely linked to land-use in the WRT River watershed: built land > agriculture > natural vegetation (Figs. S1, S2). High dissolved nitrogen concentrations are the most serious water pollution issue and followed NH$_4^+$ > NO$_3^-$ >> NO$_2^-$ (Table 1). Mean NH$_4^+$ concentration was 1.78 ± 1.86 mg/L (ranging from 0.06 to 11.14 mg/L) and constituted 57% of dissolved inorganic nitrogen. Approximately 60% and > 30% of the 95 water samples did not meet the NH$_4^+$ water quality standard Type III of 1 mg N/L (threshold for drinking water) and Type V of 2 mg N/L (minimum quality for supporting the health of aquatic ecosystem), respectively (State Environment Protection Bureau of China, 2002). The NO$_3^-$ concentrations ranged from < 0.003–3.65 mg/L, with a mean value of 1.34 $\pm$ 0.81 mg/L. NO$_2^-$ concentrations were generally low, ranging from < 0.003–0.52 mg/L. DO concentrations ranged from 0.1 to 12.2 mg/L, with 80% of samples having > 2 mg/L (a proposed threshold for hypoxic conditions facilitating microbial denitrification).

The WRT River consists of a complex river network comprising rural to highly urbanized/industrialized regions in eastern China. Due to rapid economic development and urbanization that began in the 1980 s and lagging wastewater treatment infrastructure, the rivers in eastern China receive a large amount of nutrient input from municipal/industrial/agricultural effluents. Consequently, these rivers experienced severe nutrient pollution, and many portions of the river often experience black colored, malodorous and hypoxic conditions. Black-odorous waters form in O$_2$-depleted waters/sediments when metals precipitate with

Table 1
Statistical summary of water quality parameters for quarterly sampling (4 time periods) of 24 sampling sites in the Wen-Rui Tang River network.

Parameters	N[a]	Mean	SD[b]	Minimum	Maximum	CV[c] (%)
DO (mg/L)	95	5.0	3.0	0.1	12.2	60
NH$_4^+$ (mg/L)	95	1.78	1.86	0.06	11.14	104
NO$_3^-$ (mg/L)	95	1.34	0.81	< 0.003	3.65	61
NO$_2^-$ (mg/L)	95	0.09	0.07	< 0.003	0.52	79

[a] One sample in April 2019 was missing during transport;

[b] *SD* denotes standard deviation;

[c] *CV* denotes coefficient of variation.

sulfide and stain the water black; the odorous compounds result from volatile organic and inorganic compounds generated from degradation of sulfur-containing organic matter or microbial sulfate reduction (Liang et al., 2018). Dissolved oxygen depletion results from microbial decomposition of organic materials (e.g., sewage, industrial wastes, algal biomass), as well as microbial oxidation of NH_4^+ to NO_3^- via the nitrification process.

Within the WRT River network, 92% of the river segments did not meet the Type V national water quality standard (minimum type to support aquatic ecosystem health) in 2010 (Chen et al., 2016). Given this dilemma, regulatory authorities initiated a series of strict water resource protection practices beginning in 2015 to sustain/remediate water quality and avoid further water quality deterioration. Based upon our investigation, water quality within the WRT River network has significantly improved since 2010. For example, the mean DO concentration increased from 2.5 mg/L during 2000–2010 to 5.0 mg/L, and NH_4^+ decreased from 8.07 mg/L during 2000–2010 (Mei et al., 2014) to 1.78 mg/L. Notably, the ratio of NO_3^- versus NH_4^+ increased from ~0.2 in 2010 (Ji et al., 2013) to > 0.75 in the present study, with > 55% of samples greater than 1. Considering the NH_4^+ or organic nitrogen is the predominant nitrogen form in sewage-derived effluents (Zhu et al., 2010), nitrogen fertilizer (ammonium and urea) and soil nitrogen, these sources are unlikely to directly export NO_3^- to the receiving waters. Therefore, the higher NO_3^-: NH_4^+ ratio results from greater wastewater treatment that removes/oxidizes NH_4^+, and higher DO concentrations that facilitates greater nitrification of NH_4^+ to NO_3^- within the water column. This trend highlights that NO_3^- now plays a more important role in regulating nitrogen pollution of the WRT River system than previously. These findings are consistent with other coastal plain river networks located in rapidly developing regions of eastern China where enhanced environmental protection requires a quantitative understanding of NO_3^- sources and transformations to further advance nitrogen mitigation strategies.

3.2. Nitrogen transformations as assessed by $\delta^{15}N\text{-}NO_3^-$ and $\delta^{18}O\text{-}NO_3^-$

Herein, we used the dual nitrate isotope approach to provide insights into specific nitrate sources and the dominant nitrogen-cycling processes within the WRT River watershed (Li et al., 2019; Yang and Toor, 2016). $\delta^{15}N\text{-}NO_3^-$ ranged from − 2.38–22.81‰, with a mean value of 7.38‰, and $\delta^{18}O\text{-}NO_3^-$ from − 6.9–16.56‰ with a mean value of 2.05‰. (Fig. 2). Temporal patterns for $\delta^{15}N\text{-}NO_3^-$ were 2.85–14.17‰, 4.28–12.54‰, − 2.38–16.62‰, and 2.29–22.81‰ for April, June, September and January samples, respectively. Corresponding values for $\delta^{18}O\text{-}NO_3^-$ were − 0.62–16.56‰, − 5.22–3.73‰, − 6.90–3.81‰, and − 4.17–8.76‰ in April, June, September and January, respectively. There were no distinct seasonal patterns identified for $\delta^{15}N\text{-}NO_3^-$ and $\delta^{18}O\text{-}NO_3^-$; however, April $\delta^{18}O\text{-}NO_3^-$ values were generally higher than those for the other seasons (Fig. 2). In general, the higher $\delta^{15}N\text{-}NO_3^-$ appeared in the residential regions having a higher population density and industry distribution, whereas the lower $\delta^{15}N\text{-}NO_3^-$ values were found in the agriculture and natural vegetation regions (Fig. S3). In contrast to $\delta^{15}N\text{-}NO_3^-$, $\delta^{18}O\text{-}NO_3^-$ showed an inconspicuous spatial pattern as shown in Fig. S4.

In theory, microbially-produced $\delta^{18}O\text{-}NO_3^-$ can be determined because one oxygen is derived from atmospheric O_2 and the other two oxygens are derived from ambient H_2O (Chen et al., 2020; Paredes et al., 2020; Torres-Martínez et al., 2020, 2021b; Carrey et al., 2021; Liu et al., 2021; Xuan et al., 2022). Based on the end-member $\delta^{18}O$ values of 23.50‰ and − 14.16––0.92‰ determined for atmospheric O_2 and ambient water (from nearby Fuzhou International Atomic Energy Association station, ~240 km), respectively, we estimated that microbially-produced $\delta^{18}O\text{-}NO_3^-$ should fall within the range of − 1.61–7.22‰ on the basis of $\delta^{18}O\text{-}NO_3^- = 2 \times [\delta^{18}O\text{-}H_2O]/3 + 1 \times [\delta^{18}O\text{-}O_2]/3$. However, it must be noted that $\delta^{18}O\text{-}NO_3^-$ derived from nitrification may exceed the theoretical maximum value by up to 5‰.

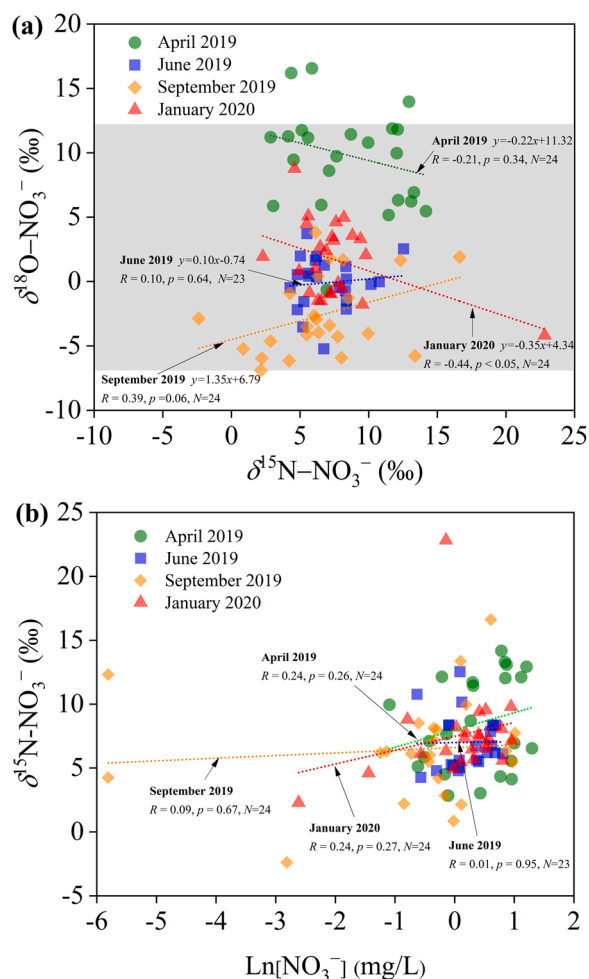**Fig. 2.** (a) Correlation diagram between $\delta^{15}N\text{-}NO_3^-$ and $\delta^{18}O\text{-}NO_3^-$ values, and (b) relationship between $\delta^{15}N\text{-}NO_3^-$ and NO_3^- concentrations. Grey rectangle represents the theoretical range for $\delta^{18}O\text{-}NO_3^-$ formed by nitrification; $\delta^{15}N\text{-}NO_3^-$ and $\delta^{18}O\text{-}NO_3^-$ values for one sample in June 2019 was not obtained due to a low nitrate content, hence $N = 23$ in June 2019.

(Kendall and McDonnell, 1998; Xue et al., 2009). In addition, the minimum $\delta^{18}O\text{-}NO_3^-$ value observed in the WRT River was − 6.90‰, which suggests that part of the $\delta^{18}O\text{-}NO_3^-$ produced from nitrification was below the theoretical range for the $\delta^{18}O\text{-}NO_3^-$ value (Snider et al., 2010). Given these constraints, the expected range of $\delta^{18}O\text{-}NO_3^-$ in the WRT River network from nitrification would fall within − 6.90–12.22‰. As displayed in Fig. 2, the measured $\delta^{18}O\text{-}NO_3^-$ values ranged from − 6.90–16.56‰, with > 90% of the values falling within the theoretical range for nitrification. Hence, we posit that the dominant source of nitrate in the WRT River watershed was produced by microbial nitrification.

Microbially denitrification is the reduction of NO_3^- to N_2, N_2O or NO under anaerobic conditions (or generally at a DO limit of < 2 mg/L) (Chen et al., 2020). During denitrification of NO_3^-, anaerobic microbes preferentially consume the light isotopes of NO_3^- (i.e., ^{14}N and ^{16}O), resulting in a simultaneous enrichment of ^{15}N and ^{18}O in the residual NO_3^-, along with a corresponding decrease in NO_3^- concentrations (Nestler et al., 2011; Hu et al., 2019; Xuan et al., 2022). Typically, the ratio of $\delta^{15}N\text{-}NO_3^-$: $\delta^{18}O\text{-}NO_3^-$ resulting from denitrification ranges from 1.3: 1–2.1: 1 (Liu et al., 2006; Torres-Martínez et al., 2020). Therefore, the slope of the $\delta^{15}N\text{-}NO_3^-$ versus $\delta^{18}O\text{-}NO_3^-$ regression line within a range of 0.48–0.77 and a significant negative relationship between $\delta^{15}N\text{-}NO_3^-$ and NO_3^- concentration provide evidence for denitrification in the system. In this study, we found no strong positive correlation

between δ^{15}N-NO$_3^-$ and δ^{18}O-NO$_3^-$, nor a negative relationship between δ^{15}N-NO$_3^-$ and NO$_3^-$ for the four sampling periods (Fig. 2). Although there was a positive correlation (R = 0.48, $p < 0.05$) existing between Ln [NO$_3^-$] and δ^{15}N-NO$_3^-$ in September 2019 without the two outlier data points at the left side of Fig. 2b, no significant positive relationship between δ^{15}N-NO$_3^-$ and δ^{18}O-NO$_3^-$ (R = 0.34, $p = 0.12$) with the expected slope value was observed (Fig. S5). We ascribe this lack of a strong denitrification signal in the WRT River network to the absence of hypoxic/anoxic conditions (mean DO was 5 mg/L) necessary to facilitate denitrification. While some denitrification may occur in anoxic sites of soils and riverine sediments, the post-denitrification NO$_3^-$ concentrations maybe insufficient to alter the overall isotopic signature owing to the high NO$_3^-$ concentrations in the water column.

3.3. Identification of main riverine NO$_3^-$ sources

We used the classical and widely used dual-NO$_3^-$ isotope cross-plot diagram to acquire qualitative information concerning the dominant riverine NO$_3^-$ source to the WRT River network (Hu et al., 2019; Taufiq et al., 2019; Torres-Martínez et al., 2020, 2021b; He et al., 2022). The cross-plot diagram of δ^{15}N-NO$_3^-$ versus δ^{18}O-NO$_3^-$ showed typical characteristics of NO$_3^-$ pollution sources originating from a mixture of soil nitrogen and municipal sewage (Fig. 3). The δ^{15}N-NO$_3^-$ versus δ^{18}O-NO$_3^-$ distribution excluded atmospheric deposition as a primary NO$_3^-$ source, in spite of a relatively high nitrate flux from atmospheric deposition (13–32 kg NO$_3$-N/ha·yr; Liao et al., 2015). This phenomenon might result from most atmospheric deposition nitrate inputs to receiving waters undergoing some biogeochemical processing within the watershed (Sebestyen et al., 2019). Nearly all the data points were distributed within the sewage dominion, with 58 points within the soil nitrogen-sewage overlap zone and 19 within the sewage zone. Accordingly, municipal sewage was identified as a possible primary source of riverine NO$_3^-$ pollution, although inputs from soil nitrogen are also likely important NO$_3^-$ sources. Combined with the previous section revealing that microbial nitrification was the main nitrogen transformation process, we infer that NH$_4^+$ originating from untreated wastewaters undergoes substantial nitrification within the river network leading to NO$_3^-$ with a high overall δ^{15}N-NO$_3^-$ signature, characteristic of a sewage origin. In summary, municipal sewage was identified as a possible important NO$_3^-$ source in the WRT River network providing water quality agencies with critical information to guide remediation practices.
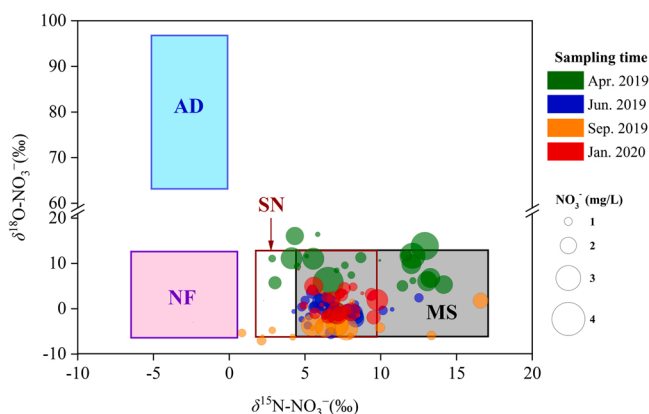
3.4. Estimation of proportional contributions from potential nitrate sources

Table 2 summarizes the specific δ^{15}N and δ^{18}O values for each expected NO$_3^-$ end-member source evaluated in this study. Accordingly, the δ^{15}N values for atmospheric deposition, nitrogen fertilizer, soil nitrogen and municipal sewage end-members were set as -2.63 ± 1.26‰, -2.25 ± 1.75‰, 5.04 ± 1.85‰, and 10.49 ± 4.53‰, respectively; corresponding δ^{18}O values were 76.83 ± 8.72‰ for atmospheric deposition, 3.45 ± 2.63‰ for municipal sewage and 4.14 ± 1.89‰ for both the nitrogen fertilizer and soil nitrogen end-members. The Wen-Rui Tang River is a large river with a mainstream length of ~34 km and tributaries/canals adding ~1200 km to the river network. In this complex watershed including soil, farmland, wetlands and riverine transformations of N, the biological processes driving N cycling were deemed sufficient to initiate significant isotopic fractionation (Denk et al., 2017; Yu et al., 2020). Thus, we incorporated ^{15}N-fractionation factors for atmospheric deposition nitrate (0‰), nitrogen fertilizer (3.9 ± 2.3‰), soil nitrogen (−4.1 ± 1.4‰) and municipal sewage (−0.6 ± 1.2‰) during the SIAR modeling process (Ostrom et al., 1998; Loo et al., 2017; Zhang et al., 2018; Ren et al., 2022).

The proportional contribution of potential nitrogen sources to riverine nitrate concentrations in the WRT River were estimated from the SIAR model (Fig. 4). Nitrate source contributions in June, September and January followed the order: municipal sewage > nitrogen fertilizer > soil nitrogen > atmospheric deposition, whereas the April contributions followed: municipal sewage > nitrogen fertilizer > atmospheric deposition ≈ soil nitrogen. Notably, the SIAR model identified municipal sewage as the likely major NO$_3^-$ pollution source with contributions ranging from 58.5% to 75.7% throughout the year. Soil nitrogen (7.8–20.1%), nitrogen fertilizer (8.6–20.9%) and atmospheric deposition (<0.1–7.9%) comprised the additional sources. The bi-plots (Fig. 3) and the SIAR model provided consistent results in identifying municipal sewage as a primary pollution source. However, the SIAR model provides a quantitative estimate of source contributions, which can not be inferred from the bi-plot method alone (Fig. 3).

Overall, the integration of isotope tracing approaches using the dual isotopes of NO$_3^-$ showed strong efficacy for evaluating nitrate pollution sources in surface waters of the WRT plain river network. The riverine NO$_3^-$ source apportionment results determined in this study were consistent with field evidence and inferences from previous water quality assessments as discussed below.

Annual domestic sewage discharge within Wenzhou was 18,232 ton N/yr in 2019 (Wenzhou Environmental Technology Inc., 2021). Today, most urban domestic sewage (>95%) is collected and transported to wastewater treatment plants for processing (Wenzhou Municipal People's Government, 2018). However, some domestic sewage/animal waste still enters the river network from sanitary and combined sewer overflows during storm events (e.g., typhoons), leakage from sewer infrastructure and runoff from animal husbandry in the rural portion of the study area. As several wastewater treatment plants do not directly

Fig. 3. Isotopic compositions of δ^{15}N-NO$_3^-$ and δ^{18}O-NO$_3^-$ for surface water samples together with typical nitrate source regions for atmospheric deposition nitrate (AD), nitrogen fertilizer (NF), soil nitrogen (SN) and municipal sewage (MS). The δ^{15}N values for MS are adapted from the nearby Changle River watershed (~160 km; Ji et al., 2017) and the other sources were measured from local pollution sources. δ^{18}O values for AD were measured from local precipitation samples and the other sources were calculated using nitrification theory.

Table 2
Isotopic characteristics (mean ± standard deviation) of suspected end-members used in the Stable Isotope Analysis in R (SIAR) model.

Source	Sampling time	N	δ^{15}N (‰)	δ^{18}O (‰)
Precipitation nitrate	April–June 2021	15	− 2.63 ± 1.26	76.83 ± 8.72
Nitrogen fertilizer	December 2020	10	− 2.25 ± 1.75	4.14 ± 1.89[a]
Soil nitrogen	December 2020	32	5.04 ± 1.85	4.14 ± 1.89[a]
Municipal sewage	—	7	10.49 ± 4.53[b]	3.45 ± 2.63[b]

[a] Data are calculated according to the δ^{18}O-O$_2$ and δ^{18}O-H$_2$O from nearby Fuzhou station (~240 km);
[b] Data obtained from the nearby Changle River watershed (~160 km; Ji et al., 2017).
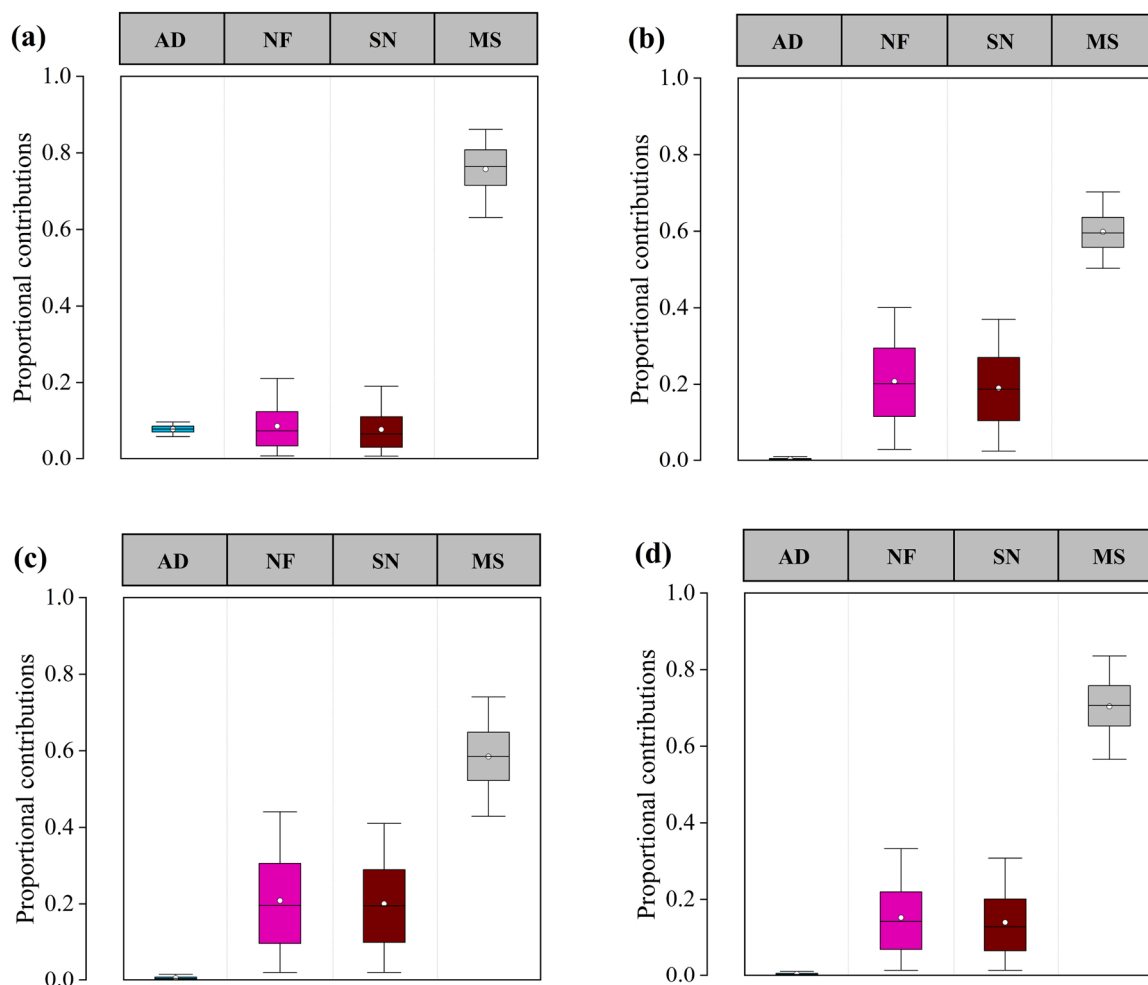
Fig. 4. Proportional contribution of potential local nitrate pollution sources in (a) April 2019, (b) June 2019, (c) September 2019, and (d) January 2020 according to the SIAR model. AD, NF, SN and MS denote atmospheric deposition nitrate, nitrogen fertilizer, soil nitrogen and municipal sewage, respectively. Box plot denotes 5th, 25th, 50th, 75th and 95th percentiles; white circles represent mean value.

discharge into the Ou River or East China Sea; a portion of the treated wastewater, which still contains high nitrogen concentrations (TN = 7–18 mg/L) and enriched in NH_4^+, is discharged into the WRT River network for ultimate transport to the ocean. This is further supported by NH_4^+ frequently being the dominant form of dissolved inorganic N in the river system, Consequently, the identification of municipal sewage as the possible major source of riverine NO_3^- by the SIAR model is fully consistent with field evidence.

High rates of nitrogen fertilization for agricultural production are common within the study region. Typical agricultural crops planted in this watershed include vegetables, fruits (e.g., melons, oranges, bayberry), sweet potato, rice, soybeans, flower gardens and tea. The application rates of N-fertilizer are ~300 kg N/ha in this region (Wenzhou Statistic Bureau, 2013) with only ~35% being absorbed by agricultural crops (Yu and Shi, 2015). This unabsorbed N-fertilizer coupled with existing soil nitrogen stocks, including legacy N accumulated in soils over time (Chen et al., 2014), is subsequently lost to the river system by rainfall-runoff and groundwater pathways. The decrease in NO_3^- sourced to fertilizer in April coincides with the beginning of the crop season (prior to fertilizer application) and the end of the dry season when antecedent runoff/leaching from agricultural lands is lowest. Given that ~40% of the watershed land area has an agricultural land use, it is not surprising that an appreciable NO_3^- load (16.4–41.0% as determined by the SIAR model) is ascribed to soil nitrogen and nitrogen fertilizer.

Atmospheric nitrogen deposition (as TN) in the study area is in the

range of 30–50 kg N/ha·yr, with the DIN component being comprised of similar amounts of NH_4^+ and NO_3^- (Liao, 2015). Thus, the contribution of atmospheric deposition is only on the order of ~15% of the fertilizer-derived nitrogen. In addition, much atmospheric nitrate infiltrates into soil and is then retained in groundwater/soil or undergoes biological processing (e.g., uptake by plants or microorganisms, dissimilatory nitrate reduction to ammonia). As a result, only a portion of the atmospheric nitrogen is transported to streams without being retained or biologically transformed (Sebestyen et al., 2019). Hence, atmospheric deposition was identified as a relatively minor source (<0.1–7.9%) of riverine NO_3^-. Subsequent studies, utilizing the $^{17}O\text{-}NO_3^-$ isotopic signature could further improve and validate the accuracy of the atmospheric nitrogen contribution (Xia et al., 2019).

3.5. Management implications for nitrate pollution remediation

Considering that municipal sewage was recognized as the primary NO_3^- source based on the SIAR model, controlling municipal sewage discharge in the WRT River watershed or other plain river networks with similar watershed characteristics would provide the most cost-effective method for riverine NO_3^- pollution attenuation. Several practical strategies are identified: (1) developing sewage collection pipeline systems to separate stormflow and sewage collection/transport to avoid release of sewage to the river system during storm events; (2) replacing deteriorating/leaking sewer pipes in older urban areas; (3) reducing runoff/leaching from animal husbandry; (4) improving wastewater treatment

processes (i.e., tertiary treatment) to reduce nitrogen concentrations of treated sewage effluents discharged to waterways; and (5) direct ocean disposal of treated wastewater versus disposal to the river system. Furthermore, soil nitrogen and nitrogen fertilizer were identified as secondary nitrate sources. Although converting farmland into forests or grasslands is able to mitigate farmland runoff and soil erosion, it is generally not a practical solution given the financial loss of agricultural commodity production. As such, the following economic practices should be considered: (1) incorporating farmland ecological ditches and vegetative buffers between farmland and rivers to reduce soil nitrogen and nitrogen fertilizer losses; and (2) encourage farmers to apply bio-based and controlled-released fertilizers based on soil fertility tests to increase N-use efficiency, thereby decreasing nitrogen fertilizer pollution. Notably, considering the stagnant nature of the WRT River during the dry season, the N inputs tend to accumulate rather than being transported (flushed) to the ocean. Thus, the use of biological floating-beds (i.e., floating wetlands) and submerged plants could be incorporated into some heavily polluted river segments to mitigate nitrogen pollution through plant uptake/harvest practices.

3.6. Uncertainty analysis

When using a modeling approach, it is important to assess the uncertainty of the projected results to demonstrate the potential margin of error associated with the simulations. We evaluated the degree of uncertainty in the nitrate source apportionment results generated by the SIAR models using UI_{90} values calculated for the contributions from each source. Additionally, to assess uncertainties induced by isotopic fractionation occurring during nitrogen transformation processes, we developed a SIAR model that did not include ^{15}N-fractionation and compared it to a model including ^{15}N-fractionation processes. As shown in Fig. 5a, the proportional contribution of atmospheric deposition nitrate was relatively stable as demonstrated by the low UI_{90} value of 0.0087, whereas larger uncertainties were associated with nitrogen fertilizer (UI_{90} = 0.32) and soil nitrogen (UI_{90} = 0.30). Municipal sewage (UI_{90} = 0.14) exhibited a moderate degree of uncertainty. By way of comparison, our UI_{90} values considering ^{15}N-fractionation

factors were lower than those in nearby Changle River watershed (eastern China; UI_{90} range = 0.06–0.62) and the Shanxi drinking water source area (eastern China; UI_{90} range = 0.08–0.67), but higher than those from Comarca Lagunera (northern Mexico; UI_{90} range = 0.05–0.24) (Ji et al., 2017; Shang et al., 2020; Torres-Martínez et al., 2021a). Notably, the SIAR model ignoring the ^{15}N-fractionation effects (fractionation factors set as zero) produced significantly greater uncertainties than comparable SIAR model incorporating ^{15}N-fractionation factors for each different N source. The UI_{90} values for atmospheric deposition nitrate, nitrogen fertilizer, soil nitrogen, and municipal sewage in the SIAR models with and without isotopic fractionation were 0.0087 vs. 0.0086, 0.32 vs. 0.25, 0.30 vs. 0.55, and 0.14 vs. 0.34, respectively (Fig. 5b). These results indicated that including isotopic fractionation factors for the different N sources within the SIAR model can significantly reduce the uncertainties and consequently improve the accuracy of the SIAR model.

Generally, the uncertainties associated with nitrate pollution source apportionment are attributable to two main factors: (1) site-specific isotope fractionation processes comprising nitrogen cycling (e.g., nitrification, denitrification, ammonia volatilization); and (2) large spatial-temporal variations of nitrate sources and their isotopic composition within a given watershed. Quantification of the fractionation degree and elucidating the initial isotopic composition of different sources at the watershed scale are important tasks, but are extremely challenging endeavors owing to the potential occurrence of multiple nitrogen transformations and the coexistence of multiple fractionation processes (e.g., equilibrium vs kinetic fractionations). This highlights the need for integrated in situ and laboratory experiments to obtain better estimates for isotopic fractionation factors of each nitrate source. Additionally, uncertainties for different pollution sources arise from the inherent uncertainty associated with the isotopic composition of end-member sources. In this study, we constrained the δ^{15}N values for the various end-members through direct measurement of several representative local sources or through the use of relevant published values from nearby locations. However, to further improve the quantitative identification of nitrate sources, it is warranted to more rigorously investigate the spatial-temporal variations in the isotopic composition of the end-
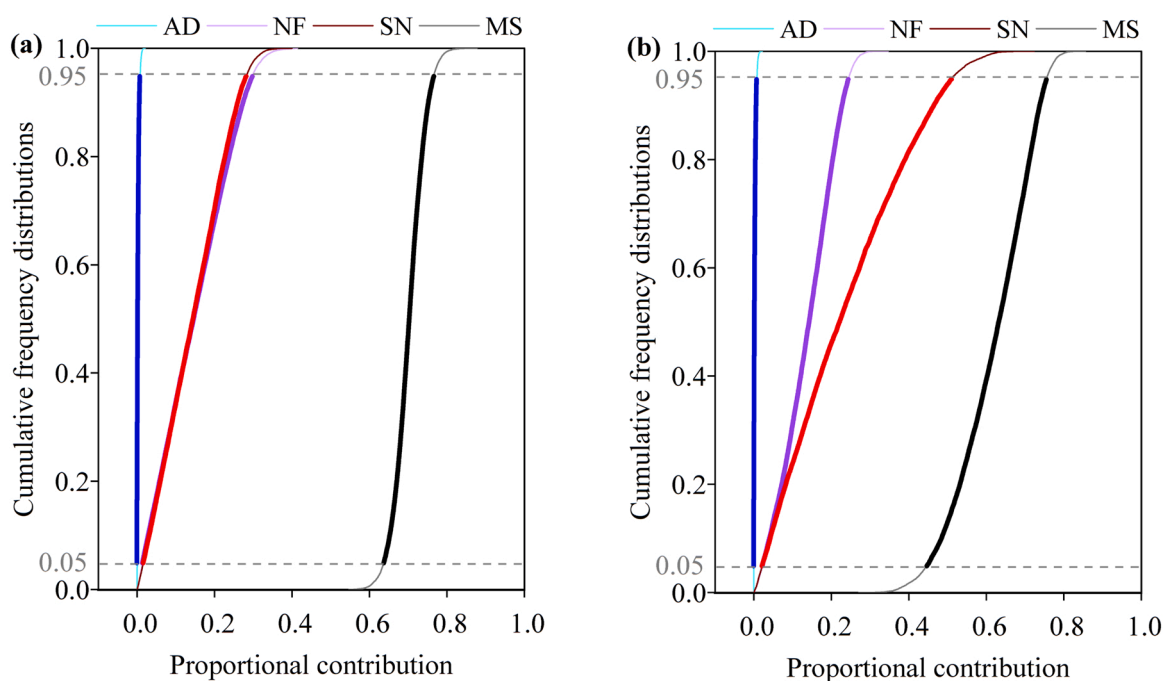

Fig. 5. Cumulative probability distributions for proportional contributions from different nitrate sources based on outputs of (a) SIAR model considering ^{15}N-fractionation and (b) SIAR model with no accounting for ^{15}N-fractionation. AD, NF, SN and MS denote atmospheric deposition nitrate, nitrogen fertilizer, soil nitrogen and municipal sewage, respectively.

member sources and the effects this variability has on modeling results.

3.7. Sensitivity analysis

The reliability of the SIAR model is closely related to the isotopic signatures of end-member pollution sources. To investigate the relative effects of source isotopic composition on modeling outputs, we performed a sensitivity analysis examining the effects of changes in input data for end-member isotopic composition on the resulting source apportionment (Fig. 6). The largest changes in source contributions resulted from differences in the mean δ^{15}N values for municipal sewage. For example, in scenario 4, the nitrogen fertilizer, soil nitrogen and municipal sewage contributions changed by ~25%, 26% and ~50%, respectively, due to variations in the mean input values of δ^{15}N for municipal sewage. In contrast, source contributions showed a moderate sensitivity to changes of soil nitrogen (scenario 3) and low sensitivity to variations in atmospheric deposition nitrate (scenario 1) and nitrogen fertilizer (scenario 2). This sensitivity analysis clearly identifies that the isotopic composition of the possible major source (i.e., municipal sewage in this study) had the strongest effect on overall results for nitrate source apportionment. Notably, the standard deviation for δ^{15}N values of municipal sewage measured in this study was the highest among the end-member sources. This highlights the necessity of accurately characterizing the isotopic signatures of pollution sources to reduce the uncertainty associated with SIAR-based nitrate source

apportionment. Given the high cost and labor associated with nutrient remediation activities, we recommend water resource managers/researchers first identify the primary pollution sources using a δ^{15}N-NO$_3^-$ versus δ^{18}O-NO$_3^-$ diagram and isotopic composition of pollution sources before investigating the site-specific isotopic composition of the possible major sources within the entire study area. These preliminary analyses will allow for targeted analyses to distinguish and quantify nitrogen source apportionment at the watershed scale.

4. Conclusions

This study integrated hydrochemistry and stable nitrate isotopes (δ^{15}N/δ^{18}O-NO$_3^-$) into a SIAR modeling framework to determine riverine nitrate contributions from four potential sources (e.g., atmospheric deposition nitrate, nitrogen fertilizer, soil nitrogen, and municipal sewage) in the Wen-Rui Tang River of eastern China. Furthermore, we quantified the uncertainties associated with nitrate source contributions and identified the sensitivity of each input end-member. Our study demonstrated that nitrate (mean = 1.34 ± 0.81 mg/L) is now an important form of nitrogen pollution in the WRT River network, as compared to ammonium being the predominant form in the past decades. Distributions of δ^{15}N/δ^{18}O-NO$_3^-$ revealed that riverine NO$_3^-$ was derived predominantly from microbial nitrification, whereas microbial denitrification was not deemed to significantly affect the isotopic composition of nitrate. The utilization of the δ^{15}N-NO$_3^-$ versus δ^{18}O-NO$_3^-$
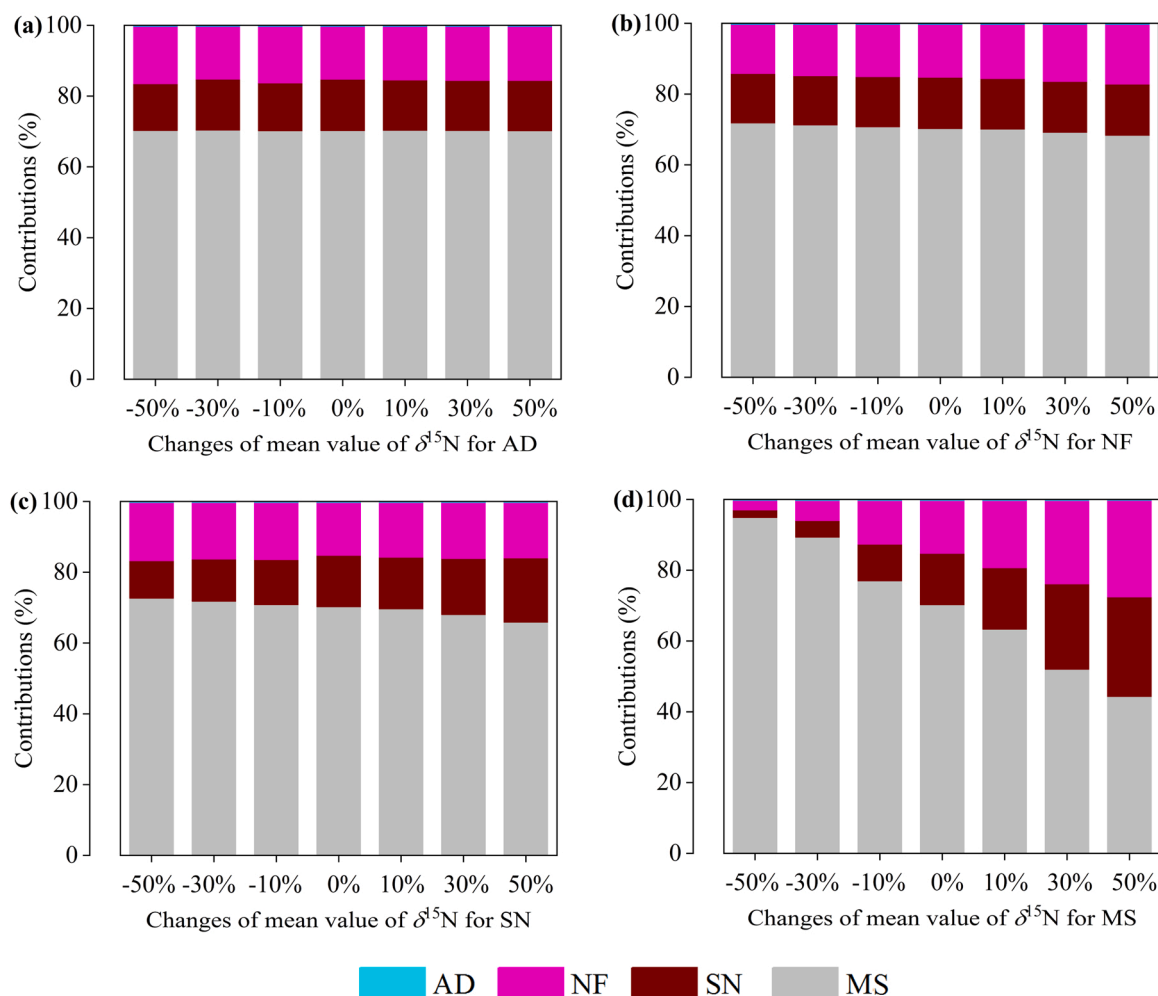

Fig. 6. Sensitivity analysis based on the perturbation method. (a) scenario 1: δ^{15}N for atmospheric deposition nitrate (AD) changed by ± 50%, ± 30%, ± 10% and 0%; (b) scenario 2: δ^{15}N for nitrogen fertilizer (NF) changed by ± 50%, ± 30%, ± 10% and 0%; (c) scenario 3: δ^{15}N for soil nitrogen (SN) changed by ± 50%, ± 30%, ± 10% and 0%; and (d) scenario 4: δ^{15}N for municipal sewage (MS) changed by ± 50%, ± 30%, ± 10% and 0%.

cross-plots and SIAR modeling identified municipal sewage as the dominant nitrate source across all four sampling seasons. SIAR modeling results demonstrated that municipal sewage contributed the most NO_3^- (58.5–75.7%) to the river network, followed by nitrogen fertilizer (8.6–20.9%), soil nitrogen (7.8–20.1%) and atmospheric deposition (<0.1–7.9%). The degree of uncertainty associated with the different pollution source contributions followed: nitrogen fertilizer ($UI_{90} = 0.32$) > soil nitrogen ($UI_{90} = 0.30$) > municipal sewage ($UI_{90} = 0.14$) > atmospheric deposition nitrate ($UI_{90} = 0.0087$). Model sensitivity analysis identified the isotopic composition of the major source (i.e., municipal sewage) as the most sensitive model input variable. Overall, the comprehensive isotope tracing approach utilized in this study provided an efficient and effective tool to guide nitrate pollution control and remediation of river networks at the watershed scale. However, it must be acknowledged that isotopic fractionation during nitrogen cycling processes was not explicitly considered in this study. Further work should focus on conducting in situ and laboratory experiments to better quantify the ^{15}N isotopic fractionation effects associated with different nitrogen transformations. Furthermore, it is warranted to apply the conservative oxygen isotope, known as anomalous ^{17}O enrichment ($\triangle^{17}O$), which provides an independent assessment of atmospheric nitrate and terrestrial source contributions as it does not change during biogeochemical transformations. Incorporation of $\triangle^{17}O$ will reduce ^{18}O fractionation uncertainties, thereby improving the accuracy of nitrate source apportionment results. In addition, it is recommended to collect ancillary water quality and GIS data for developing alternative modeling results (e.g., Chemical Mass Balance model, SWAT model) to serve as a measure of cross-validation with the SIAR isotopic method.

CRediT authorship contribution statement

Xiaoliang Ji: Conceptualization, Methodology, Formal analysis, Investigation, Visualization, Writing – original draft, Writing – review & editing. **Lielin Shu:** Investigation, Writing – review & editing. **Wenli Chen:** Investigation. **Zheng Chen:** Methodology, Investigation. **Xu Shang:** Conceptualization, Investigation. **Yue Yang:** Conceptualization, Supervision, Methodology, Formal analysis, Investigation, Writing – original draft. **Randy A. Dahlgren:** Conceptualization, Methodology, Writing-original draft, Writing – review & editing. **Minghua Zhang:** Supervision, Writing-original draft, Writing – review & editing, Funding acquisition.

Ethical approval

Not applicable.

Consent to participate

Not applicable.

Consent to publish

Not applicable.

Competing interests

The authors declare no competing financial interests.

Statement of environmental implication

Nitrate is a hazardous material contributing to human health risks and eutrophication/hypoxia/harmful algae blooms in aquatic ecosystems. Nowadays, $\delta^{15}N/\delta^{18}O$-$NO_3^-$-based SIAR modeling is widely employed to identify riverine nitrate sources. However, the effect of variations in nitrogen-source isotopic composition on nitrate-source contributions when using SIAR models has not been previously investigated. In this study, we estimated contributions from various nitrate sources and quantified their uncertainties. Importantly, we investigated the sensitivity of each input end-member for the first time, which complemented our understanding of riverine nitrate source contributions.

Declaration of Competing Interest

The authors declare that they have no known competing financial interests or personal relationships that could have appeared to influence the work reported in this paper.

Data Availability

All data generated or analyzed during this study are included in this published article.

Appendix A. Supporting information

Supplementary data associated with this article can be found in the online version at doi:10.1016/j.jhazmat.2022.129480.

References

Arnold, J.G., Fohrer, N., 2005. SWAT2000: current capabilities and research opportunities in applied watershed modelling. Hydrol. Process. 19, 563–572. https://doi.org/10.1002/hyp.5611.

Biddau, R., Cidu, R., Da Pelo, S., Carletti, A., Ghiglieri, G., Pittalis, D., 2019. Source and fate of nitrate in contaminated groundwater systems: assessing spatial and temporal variations by hydrogeochemistry and multiple stable isotope tools. Sci. Total Environ. 647, 1121–1136. https://doi.org/10.1016/j.scitotenv.2018.08.007.

Burow, K.R., Nolan, B.T., Rupert, M.G., Dubrovsky, N.M., 2010. Nitrate in groundwater of the United States, 1991-2003. Environ. Sci. Technol. 44, 4988–4997. https://doi.org/10.1021/es100546y.

Carey, R.O., Migliaccio, K.W., Brown, M.T., 2011. Nutrient discharges to Biscayne Bay, Florida: trends, loads, and a pollutant index. Sci. Total Environ. 409, 530–539. https://doi.org/10.1016/j.scitotenv.2010.10.029.

Carrey, R., Ballesté, E., Blanch, A.R., Lucena, F., Pons, P., López, J.M., Rull, M., Solà, J., Micola, N., Fraile, J., Garrido, T., Munné, A., Soler, Otero, N., 2021. Combining multi-isotopic and molecular source tracking methods to identify nitrate pollution sources in surface and groundwater. Water Res. 188, 116537 https://doi.org/10.1016/j.watres.2020.116537.

Casciotti, K.L., Sigman, D.M., Hastings, M.G., Bohlke, J.K., Hilkert, A., 2002. Measurement of the oxygen isotopic composition of nitrate in seawater and freshwater using the denitrifier method. Anal. Chem. 74, 4905–4912. https://doi.org/10.1021/ac020113w.

Chen, D.J., Huang, H., Hu, M.P., Dahlgren, R.A., 2014. Influence of lag effect, soil release, and climate change on watershed anthropogenic nitrogen inputs and riverine export dynamics. Environ. Sci. Technol. 48, 5683–5690. https://doi.org/10.1021/es500127t.

Chen, Q., Mei, K., Dahlgren, R.A., Wang, T., Gong, J., Zhang, M., 2016. Impacts of land use and population density on seasonal surface water quality using a modified geographically weighted regression. Sci. Total Environ. 572, 450–466. https://doi.org/10.1016/j.scitotenv.2016.08.052.

Chen, X., Jiang, C., Zheng, L., Dong, X., Chen, Y., Li, C., 2020. Identification of nitrate sources and transformations in basin using dual isotopes and hydrochemistry combined with a Bayesian mixing model: application in a typical mining city. Environ. Pollut. 267, 115651 https://doi.org/10.1016/j.envpol.2020.115651.

Denk, T.R.A., Mohn, J., Decock, C., Lewicka-Szczebak, D., Harris, E., Butterbach-Bahl, K., Kiese, R., Wolf, B., 2017. The nitrogen cycle: a review of isotope effects and isotope modeling approaches. Soil Biol. Biochem. 105, 121–137. https://doi.org/10.1016/j.soilbio.2016.11.015.

Divers, M.T., Elliott, E.M., Bain, D.J., 2014. Quantification of nitrate sources to an urban stream using dual nitrate isotopes. Environ. Sci. Technol. 48, 10580–10587. https://doi.org/10.1021/es404880j.

Donigian, A., Imhoff, J., Bicknell, B., Kittle, J., 1984. Application guide for the Hydrological Simulation Program Fortran. GA7 Environmental Research Laboratory, US Environmental Protection Agency, Athens.

He, S., Li, P., Su, F., Wang, Dan, Ren, X., 2022. Identification and apportionment of shallow groundwater nitrate pollution in Weining Plain, northwest China, using hydrochemical indices, nitrate stable isotopes, and the new Bayesian stable isotope mixing model (MixSIAR). Environ. Pollut. 298, 118852 https://doi.org/10.1016/j.envpol.2022.118852.

Hord, N.G., 2011. Dietary nitrates, nitrites, and cardiovascular disease. Curr. Atheroscler. Rep. 13, 484–492. https://doi.org/10.1007/s11883-011-0209-9.

Hu, M., Liu, Y., Zhang, Y., Dahlgren, R.A., Chen, D., 2019. Coupling stable isotopes and water chemistry to assess the role of hydrological and biogeochemical processes on riverine nitrogen sources. Water Res. 150, 418–430. https://doi.org/10.1016/j.watres.2018.11.082.

Ji, X., Xie, R., Hao, Y., Lu, J., 2017. Quantitative identification of nitrate pollution sources and uncertainty analysis based on dual isotope approach in an agricultural watershed. Environ. Pollut. 229, 586–594. https://doi.org/10.1016/j.envpol.2017.06.100.

Ji, X., Zhu, Y., Shang, X., Zhang, M., 2013. Spatiotemporal variation and assessment of water quality in Wen-Rui Tang River network areas. Res. Soil & Water Conse. 20, 241–246. (in Chinese).

Jin, Z., Zheng, Q., Zhu, C., Wang, Y., Cen, J., Li, F., 2018. Contribution of nitrate sources in surface water in multiple land use areas by combining isotopes and a Bayesian isotope mixing model. Appl. Geochem. 93, 10–19. https://doi.org/10.1016/j.apgeochem.2018.03.014.

Jin, Z.X., Wang, J.F., Chen, J.A., Zhang, R.X., Li, Y., Lu, Y.T., He, K.K., 2020. Identifying the sources of nitrate in a small watershed using $\delta^{15}N$-$\delta^{18}O$ isotopes of nitrate in the Kelan Reservoir, Guangxi, China. Agric. Agr. Ecosyst. Environ. 297, 106936 https://doi.org/10.1016/j.agee.2020.106936.

Johnes, P.J., 1996. Evaluation and management of the impact of land use change on the nitrogen and phosphorus load delivered to surface waters: The export coefficient modelling approach. J. Hydrol. 183, 323–349. https://doi.org/10.1016/0022-1694(95)02951-6.

Ju, Y., Mahlknecht, J., Lee, K.K., Kaown, D., 2022. Bayesian approach for simultaneous recognition of contaminant sources in groundwater and surface-water resources. Curr. Opin. Environ. Sci. Health 25, 100321. https://doi.org/10.1016/j.coesh.2021.100321.

Kendall, C., McDonnell, J.J., 1998. Isotope Tracers in Catchment Hydrology. Elsevier, Amsterdam.

Kendall, C., Elliott, E.M., Wankel, S.D., 2007. Tracing anthropogenic inputs of nitrogen to ecosystems. Stable Isotopes in Ecology and Environmental Science, second ed. Blackwell Publishing Ltd., pp. 375–449. https://doi.org/10.1002/9780470691854.ch12.

Li, C., Li, S.L., Yue, F.J., Liu, J., Zhong, J., Yan, Z.F., Zhang, R.C., Wang, Z.J., Xu, S., 2019. Identification of sources and transformations of nitrate in the Xijiang River using nitrate isotopes and Bayesian model. Sci. Total Environ. 646, 801–810. https://doi.org/10.1016/j.scitotenv.2018.07.345.

Liang, Z.W., Siegert, M., Fang, W.W., Sun, Y., Jiang, F., Lu, H., Chen, G.H., Wang, S.Q., 2018. Blackening and odorization of urban rivers: a bio-geochemical process. FEMS Microbiol. Ecol. 94, fix180. https://doi.org/10.1093/femsec/fix180.

Liao, Z., Li, P., Shang, X., 2015. Difference between urban and rural of atmospheric nitrogen and phosphorus deposition in typical areas of Wenzhou. Zhejiang Agr. Sci. 56, 123–126 (in Chinese).

Loo, S.E., Ryan, M.C., Zebarth, B.J., Kuchta, S.H., Neilsen, D., Mayer, B., 2017. Use of $\delta^{15}N$ and $\delta^{18}O$ values for nitrate source identification under irrigated crops: a cautionary vadose zone tale. J. Environ. Qual. 46, 528–536. https://doi.org/10.2134/jeq2016.08.0294.

Mayer, B., Bollwerk, S.M., Mansfeldt, T., Hutter, B., Veizer, J., 2001. The oxygen isotope composition of nitrate generated by nitrification in acid forest floors. Geochim. Cosmochim. Acta 65, 2743–2756. https://doi.org/10.1016/S0016-7037(01)00612-3.

Mei, K., Liao, L.L., Zhu, Y.L., Lu, P., Wang, Z.F., Dahlgren, R.A., Zhang, M.H., 2014. Evaluation of spatial-temporal variations and trends in surface water quality across a rural-suburban-urban interface. Environ. Sci. Pollut. Res. 21, 8036–8051. https://doi.org/10.1007/s11356-014-2716-z.

Paredes, I., Otero, N., Soler, A., Green, A.J., 2020. Agricultural and urban delivered nitrate pollution input to Mediterranean temporary freshwaters. Agr. Ecosyst. Environ. 294, 106859 https://doi.org/10.1016/j.agee.2020.106859.

Ren, K., Pan, X., Yuan, D., Zeng, J., Liang, J., Peng, C., 2022. Nitrate sources and nitrogen dynamics in a karst aquifer with mixed nitrogen inputs (Southwest China): revealed by multiple stable isotopic and hydro-chemical proxies. Water Res. 210, 118000 https://doi.org/10.1016/j.watres.2021.118000.

Rossman, L.A., 2015. Storm water management model user's manual version 5.1. ⟨https://www.epa.gov/sites/production/files/2019–02/documents/epaswmm5_1_manual_master_8–2-15.pdf⟩.

Sigman, D.M., Casciotti, K.L., Andreani, M., Barford, C., Galanter, M., Bohlke, J.K., 2001. A bacterial method for the nitrogen isotopic analysis of nitrate in seawater and freshwater. Anal. Chem. 73, 4145–4153. https://doi.org/10.1021/ac010088e.

Snider, D.M., Spoelstra, J., Schiff, S.L., Venkiteswaran, J.J., 2010. Stable oxygen isotope ratios of nitrate produced from nitrification: 18O-labeled water incubations of agricultural and temperate forest soils. Environ. Sci. Technol. 44, 5358–5364. https://doi.org/10.1021/es1002567.

State Environment Protection Bureau of China, 2002. Environmental Quality Standards for Surface Water. China Environmental Science Press, Beijing (in Chinese).

Liao, Z., 2015. Study on the contamination of atmospheric nitrogen deposition in Wenzhou region. Wenzhou medical university, Wenzhou, Zhejiang, China. (in Chinese).

Liu, C.Q., Li, S.L., Lang, Y.C., Xiao, H.Y., 2006. Using $\delta^{15}N$- and $\delta^{18}O$-values to identify nitrate sources in karst ground water, Guiyang, Southwest China. Environ. Sci. Technol. 40, 6928–6933. https://doi.org/10.1021/es0610129.

Liu, T., Wang, F., Michalski, G., Xia, X., Liu, S., 2013. Using ^{15}N, ^{17}O, and ^{18}O to determine nitrate sources in the Yellow River, China. Environ. Sci. Technol. 47, 13412–13421. https://doi.org/10.1021/es403357m.

Liu, X.L., Han, G., Zeng, J., Liu, M., Li, X.Q., 2021. Identifying the sources of nitrate contamination using a combined dual isotope, chemical and Bayesian model approach in a tropical agricultural river: case study in the Mun River, Thailand. Sci. Total Environ. 760, 143938 https://doi.org/10.1016/j.scitotenv.2020.143938.

Lu, L., Cheng, H., Pu, X., Liu, X., Cheng, Q., 2015. Nitrate behaviors and source apportionment in an aquatic system from a watershed with intensive agricultural activities. Environ. Sci. Proc. Imp. 17, 131–144. https://doi.org/10.1039/C4EM00502C.

Nestler, A., Berglund, M., Accoe, F., Duta, S., Xue, D., Boeckx, P., Taylor, P., 2011. Isotopes for improved management of nitrate pollution in aqueous resources: review of surface water field studies. Environ. Sci. Pollut. Res. 18, 519–533. https://doi.org/10.1007/s11356-010-0422-z.

Ostrom, N.E., Knoke, K.E., Hedin, L.O., Robertson, G.P., Smucker, A.J.M., 1998. Temporal trends in nitrogen isotope values of nitrate leaching from an agricultural soil. Chem. Geol. 146, 219–227. https://doi.org/10.1016/S0009-2541(98)00012-6.

Parnell, A.C., Inger, R., Bearhop, S., Jackson, A.L., 2010. Source portioning using stable isotopes: coping with too much variation. PLoS One 5, e9672. https://doi.org/10.1371/journal.pone.0009672.

Sebestyen, S.D., Ross, D.S., Shanley, J.B., Elliott, E.M., Kendall, C., Campbell, J.L., Dail, D.B., Fernandez, I.J., Goodale, C.L., Lawrence, G.B., Lovett, G.M., McHale, P.J., Mitchell, M.J., Nelson, S.J., Shattuck, M.D., Wickman, T.R., Barnes, R.T., Bostic, J.T., Buda, A.R., Burns, D.A., Eshleman, K.N., Finlay, J.C., Nelson, D.M., Ohte, N., Pardo, L.H., Rose, L.A., Sabo, R.D., Schiff, S.L., Spoelstra, J., Williard, K.W.J., 2019. Unprocessed atmospheric nitrate in waters of the Northern Forest Region in the US and Canada. Environ. Sci. Technol. 53 (7), 3620–3633. https://doi.org/10.1021/acs.est.9b01276.

Shang, X., Huang, H., Mei, K., Xia, F., Chen, Z., Yang, Y., Dahlgren, R.A., Zhang, M.H., Ji, X.L., 2020. Riverine nitrate source apportionment using dual isotopes in a drinking water source watershed of southeast China. Sci. Total Environ. 724, 137975 https://doi.org/10.1016/j.scitotenv.2020.137975.

Smith, R.A., Schwarz, G.E., Alexander, R.B., 1997. Regional interpretation of water-quality monitoring data. Water Resour. Res. 33, 2781–2798. https://doi.org/10.1029/97WR02171.

Soto, D.X., Koehler, G., Wassenaar, L.I., Hobson, K.A., 2019. Spatio-temporal variation of nitrate sources to Lake Winnipeg using N and O isotope ($\delta^{15}N$, $\delta^{18}O$) analyses. Sci. Total Environ. 647, 486–493. https://doi.org/10.1016/j.scitotenv.2018.07.346.

Taufiq, A., Effendi, A.J., Iskandar, I., Hosono, T., Hutasoit, L.M., 2019. Controlling factors and driving mechanisms of nitrate contamination in groundwater system of Bandung Basin, Indonesia, deduced by combined use of stable isotope ratios, CFC age dating, and socioeconomic parameters. Water Res. 148, 292–305. https://doi.org/10.1016/j.watres.2018.10.049.

Torres-Martínez, J.A., Mora, A., Knappett, P.S.K., Ornelas-Soto, N., Mahlknecht, J., 2020. Tracking nitrate and sulfate sources in groundwater of an urbanized valley using a multi-tracer approach combined with a Bayesian isotope mixing model. Water Res. 182, 115962 https://doi.org/10.1016/j.watres.2020.115962.

Torres-Martínez, J.A., Mora, A., Mahlknecht, J., Daesle, L.W., Cervantes-Aviles, P.A., Ledesma-Ruiz, R., 2021a. Estimation of nitrate pollution sources and transformations in groundwater of an intensive livestock-agricultural area (Comarca Lagunera), combining major ions, stable isotopes and MixSIAR model. Environ. Pollut. 269, 115445 https://doi.org/10.1016/j.envpol.2020.115445.

Torres-Martínez, J.A., Mora, A., Mahlknecht, J., Kaown, D., Barceló, D., 2021b. Determining nitrate and sulfate pollution sources and transformations in a coastal aquifer impacted by seawater intrusion-A multi-isotopic approach combined with self-organizing maps and a Bayesian mixing model. J. Hazard. Mater. 417, 126103 https://doi.org/10.1016/j.jhazmat.2021.126103.

Wang, W., Chen, L., Shen, Z., 2020a. Dynamic export coefficient model for evaluating the effects of environmental changes on non-point source pollution. Sci. Total Environ. 747, 141164 https://doi.org/10.1016/j.scitotenv.2020.141164.

Wang, Y., Peng, J.F., Gao, X.F., Xu, Y., Yu, H.W., Duan, G.Q., Qu, J.H., 2020b. Isotopic and chemical evidence for nitrate sources and transformation processes in a plateau lake basin in Southwest China. Sci. Total Environ. 711, 134856 https://doi.org/10.1016/j.scitotenv.2019.134856.

Wang, Z., Su, B., Xu, X., Di, D., Huang, H., Mei, K., Dahlgren, R.A., Zhang, M., Shang, X., 2018. Preferential accumulation of small (<300 μm) microplastics in the sediments of a coastal plain river network in eastern China. Water Res. 144, 393–401. https://doi.org/10.1016/j.watres.2018.07.050.

Wenzhou Statistic Bureau, 2013. Wenzhou Statistical Yearbook. China Statistic Press, Beijing, China (in Chinese).

Wenzhou Environmental Technology Inc., 2021. Self-assessment report on total nitrogen control in Wenzhou during the 13th Five Year Plan Period. (in Chinese).

Wenzhou Municipal People's Government, 2018. Wenzhou Yearbook. Publishing House of Local Records, Beijing, China. (in Chinese).

World Health Organization, 2011. Guidelines for drinking-water quality. 4rd ed. Geneva.

Xia, X., Li, S., Wang, F., Zhang, S., Fang, Y., Li, J., Michalski, G., Zhang, L., 2019. Triple oxygen isotopic evidence for atmospheric nitrate and its application in source identification for river systems in the Qinghai-Tibetan Plateau. Sci. Total Environ. 688, 270–280. https://doi.org/10.1016/j.scitotenv.2019.06.204.

Xuan, Y., Liu, G., Zhang, Y., Cao, Y., 2022. Factor affecting nitrate in a mixed land-use watershed of southern China based on dual nitrate isotopes, sources or

transformations? J. Hydrol. 604, 127220 https://doi.org/10.1016/j.
jhydrol.2021.127220.

Xue, D., Botte, J., De Baets, B., Accoe, F., Nestler, A., Taylor, P., Van Cleemput, O.,
Berglund, M., Boeckx, P., 2009. Present limitations and future prospects of stable
isotope methods for nitrate source identification in surface- and groundwater. Water
Res. 43, 1159–1170. https://doi.org/10.1016/j.watres.2008.12.048.

Xue, D., De Baets, B., Van Cleemput, O., Hennessy, C., Berglund, M., Boeckx, P., 2012.
Use of a Bayesian isotope mixing model to estimate proportional contributions of
multiple nitrate sources in surface water. Environ. Pollut. 161, 43–49. https://doi.
org/10.1016/j.envpol.2011.09.033.

Yang, L.P., Han, J.P., Xue, J.L., Zeng, L.Z., Shi, J.C., Wu, L.S., 2013. Nitrate source
apportionment in a subtropical watershed using Bayesian model. Sci. Total Environ.
463, 340–347. https://doi.org/10.1016/j.scitotenv.2013.06.021.

Yang, Y.Y., Toor, G.S., 2016. δ^{15}N and δ^{18}O reveal the sources of nitrate-nitrogen in
urban residential stormwater runoff. Environ. Sci. Technol. 50, 2881–2889. https://
doi.org/10.1021/acs.est.5b05353.

Yu, F., Shi, W.M., 2015. Nitrogen use efficiencies of major grain crops in China in recent
10 years. Acta Pedol. Sin. 52, 1311–1324 (in Chinese).

Yu, L., Zheng, T., Zheng, X., Hao, Y., Yuan, R., 2020. Nitrate source apportionment in
groundwater using Bayesian isotope mixing model based on nitrogen isotope
fractionation. Sci. Total Environ. 718, 137242 https://doi.org/10.1016/j.
scitotenv.2020.137242.

Zhang, M., Zhi, Y., Shi, J., Wu, L., 2018. Apportionment and uncertainty analysis of
nitrate sources based on the dual isotope approach and a Bayesian isotope mixing
model at the watershed scale. Sci. Total Environ. 639, 1175–1187. https://doi.org/
10.1016/j.scitotenv.2018.05.239.

Zhu, H., Li, H.Z., Ye, J.F., Fu, W., 2010. Coefficients of major pollutants in domestic
sewage in Shanghai. China Environ. Sci. 30, 37–41 (in Chinese).